



INTERNATIONAL ATOMIC ENERGY AGENCY
 OECD NUCLEAR ENERGY AGENCY



INTERNATIONAL SYMPOSIUM ON OCCUPATIONAL RADIATION EXPOSURE
 IN NUCLEAR FUEL CYCLE FACILITIES

Los Angeles, USA, 18-22 June 1979

IAEA-SM-242/ 24

STRAY NEUTRON FIELDS IN THE CONTAINMENT OF PWRs

Ferenc Hajnal

Environmental Measurements Laboratory
 U. S. Department of Energy
 New York, NY 10014

*With the compliments of the
 Environmental Measurements Laboratory*

Ferenc Hajnal

UNITED STATES
 DEPARTMENT OF ENERGY
 ENVIRONMENTAL MEASUREMENTS LABORATORY
 376 HUDSON STREET
 NEW YORK, N. Y. 10014

Oral Presentation

POOR ORIGINAL

8001160 930

P

This is a preprint of a paper intended for presentation at a scientific meeting. Because of the provisional nature of its content and since changes of substance or detail may have to be made before publication, the preprint is made available on the understanding that it will not be cited in the literature or in any way be reproduced in its present form. The views expressed and the statements made remain the responsibility of the named author(s); the views do not necessarily reflect those of the government of the designating Member State(s) or of the designating organization(s). In particular, neither the IAEA nor any other organization or body sponsoring this meeting can be held responsible for any material reproduced in this preprint.

1. INTRODUCTION

There have been few systematic investigations of the stray penetrating radiation fields to which workers and instruments are exposed inside the containments of nuclear power reactors. The recent concern about neutron exposure in these mixed field inside pressurized water reactor containments and how adequately neutrons are routinely monitored has motivated the development of data needed to evaluate the distribution of doses to workers and to determine levels of exposure⁽¹⁾.

Gamma radiation monitoring of operations and maintenance staff is performed relatively easily. The determination of neutron dose or dose-equivalent values and their distributions with neutron energy in the presence of significant gamma-ray levels inside and near PWR containments with available instrumentation is more difficult. The unpleasant if not hostile conditions of high ambient temperature and humidity and possible airborne and surface radionuclide contamination are barriers to the required spectrometric investigations.

Recently, measurements have been made with various devices, such as low energy resolution, moderating sphere systems and with fission counters using ^{235}U , ^{238}U and ^{237}Np in conjunction with various thermal neutron absorbers^(2,3). Polycarbonate track etch detectors with ^{238}U , ^{237}Np and ^{239}Pu fission foils also have been used to measure neutron flux and to obtain dose-equivalent rates⁽⁴⁾.

The present paper reports some results of a collaborative study performed in the containments of six PWR's of somewhat different design and construction. Both passive LiF thermoluminescence detectors (TLD) and active LiI(Eu) scintillators were employed as thermal neutron detectors with the multisphere neutron spectrometer systems. The total neutron flux and dosimetric quantities, such as absorbed dose and dose equivalent, as well as values of average energy, \bar{E} , and quality factor, QF, were obtained from the spectral determinations. Tentatively, the results indicate that rapid estimates of quality factors and average energies may be obtained, from the ratios of measurements performed with different moderator spheres⁽⁵⁾.

2. THE MULTISPHERE NEUTRON SPECTROMETER SYSTEM

A multisphere neutron spectrometry system was used in the experiments⁽⁶⁾.

Six different diameter (2, 3, 5, 8, 10 and 12 in.) polyethylene moderating spheres along with a bare neutron detector and one covered with a 0.032 in. thick cadmium absorber form the system. The neutron detectors are paired ^6LiF and ^7LiF TLD's, and 4 x 4 mm and 12.7 x 12.7 mm cylindrical $^6\text{LiI(Eu)}$ scintillators. The energy response functions of the detectors were calculated in 26 evenly spaced logarithmic intervals from thermal to 26 MeV.

Each thermoluminescence detector has four each of ^6LiF and ^7LiF chips stacked to form two separate 3.2 x 3.2 x 3.6 mm columns, whose surface areas are the same as that of the equivalent sphere used in the calculations of the 4 x 4 mm right cylindrical scintillator response function. The net signal due to the ^6Li (n, α) reactions are extracted from the TLD measurements after individual chip responses are corrected for observed loss of sensitivity due to neutron irradiation damage. The TLD stacks were positioned inside the cadmium covers in the same geometry to minimize readout differences due to the neutron capture gamma radiation from the cadmium. The 4 x 4 mm ^6Li responses, after normalization, were used in unfolding both types of spectrometric measurements.

The use of highly enriched $^6\text{LiI(Eu)}$ scintillator results in good resolution (about 9 percent) and in high light output which makes gamma-ray background differentiation relatively easy and reliable. In practice, the measurements are recorded on a multi-channel analyzer and the background as represented by the area remaining after a straight line background under the neutron peak is subtracted.

The measurements were unfolded with an iterative unfolding method that successively corrects trial solutions finding only non-negative values, while the deviation between the measured and computed detector responses is minimized⁽⁷⁾. It is inherent of iterative least-squares unfolding techniques that sometimes only a reasonably smooth unfolded spectrum can be obtained from measurements with poor statistics. Care must be taken to assure that the measurement is good before the unfolded spectrum is accepted. Tests

are being made to resolve this problem, but reliance on inter-laboratory comparison measurements is necessary at present.

3. REACTOR MEASUREMENT METHODS

The measurements in the containments of the PWR's were usually made at one meter from the floor level. Data were acquired by switching moderator spheres between the two scintillators, and the acquisition of a complete data set of two spectra required about 30 minutes. Data acquisition with the TLD system required a minimum of several hours, while in low neutron fields, the TLD system was exposed for two or three days.

The scintillation detectors performed very well in gamma-ray fields up to tens of mrad/h combined with neutron contributions of hundreds of mrem/h. The 4 x 4 mm scintillator was more useful for higher neutron dose rates and the 12.7 x 12.7 mm scintillator in higher gamma-ray dose rate fields.

As mentioned earlier, data from the active system were accumulated with a multi-channel analyzer and stored on magnetic tape for later analysis. Due to high ambient temperature and humidity in the containment, the electronics were enclosed in an insulated, air tight container cooled with dry ice and dried with silica gel. The dry ice kept the inside temperature below about 40°C for two days, and the closed container protected the instrumentation from contamination.

4. RESULTS AND DISCUSSION

SLIDE #1

The energy spectra derived by unfolding the multisphere measurements were used to calculate the integral quantities, such as neutron flux, ϕ , average energy (\bar{E}), absorbed dose and dose-equivalent rate and quality factor (QF). We shall show only one example, Figure 1, of the differential energy spectra, measured on the operating floor near the reactor cavity and the control drive mechanism. This neutron spectrum is relatively "hard"; \bar{E} is 90 keV and the quality factor is 6.4. The absorbed dose rate is 3 mrad/h, the dose-equivalent rate is 19 mrem/h, and the total neutron flux is 1060 n/cm² s. Eighteen percent of the neutrons are thermal and about 13 percent have energies greater than

300 keV, that is over the threshold energy of the track etch detectors⁽⁸⁾. Generally, the differential energy spectra have thermal groups of various intensities followed by an approximately 1/E distribution. Then, depending on the \bar{E} and QF, the spectra may decline rapidly. In the case of $\bar{E} = 7$ keV, for example, a rapid decline sets in at about 4 keV and virtually no neutrons are found over 200 keV.

The 30 spectral measurements have a wide range of \bar{E} , from 0.4 keV to about 1 MeV, with the \bar{E} of 26 of these measurements being from 10 keV to 1 MeV. The single $\bar{E} > 1$ MeV measurement point has a spurious peak in the unfolded spectrum at about 10 MeV, which might be attributed to the limitation of the unfolding procedure.

SLIDE #2

The quality factor distribution showed two peaks; 24 were from 4 to 7 and 6 from 2 to 3 as shown in Figure 2. Larger quality factors were dominant on the top or operating floor and somewhat small values, $QF < 3$, for the middle levels of the reactors. For the very large \bar{E} change, from 0.1 to 100 keV, the quality factor changes only from 2 to 4. For the 24 measurements which have QF equal to 4-7, \bar{E} changes only from 40 keV to 1 MeV. The neutron flux varies moderately, from 2.5×10^2 to 2.6×10^4 n/(cm² s). No unusually high thermal or fast flux fields were encountered.

To extract the kind of information from the measurements which might help us to understand the in containment stray neutron fields of the PWR's we used graphical and correlation analysis techniques. The graphical display of the measured and evaluated data aided us in understanding the numerical relationships reflected in the data. This method helped us to reveal of some peculiarities in the observed data and helped us to identify subsets. The graphical data display uncovered features of the data that were totally unanticipated prior to the data analysis. Generally, the absence of precedents of dealing with reactor measurements, the graphical representation of the data was chosen on trial and error basis, until representations have been found which seemingly simplified the data and seemed good candidates for correlation analysis. The data were plotted and crossplotted in various ways using the total flux, \bar{E} , QF, specific dose, specific dose equivalent, sphere responses, sphere response ratios, their products or their ratios as variables.

SLIDE #3

The logarithm of the specific dose equivalent, rem per n/cm^2 , versus the quality factor QF exhibits a linear dependence as shown in Figure 3. The two points on the top of the graph at 3.5 and 3.6×10^{-8} rem per n/cm^2 (QF are 3.9 and 9.1) were measured with our primary detector, a 12.7×12.7 mm LiI(Eu) scintillator detector in low scattering environment. The measures \bar{E} are 2.8 and 2.6 MeV. The theoretical values for bare ^{252}Cf sources are $\bar{E} = 2.13$ MeV and $QF = 9.3$. There appears to be two subsets, the reactor measurements plus the D_2O moderated ^{252}Cf source form one subset and the rest of the calibration sources form the second subset. This kind of separation even more pronounced if \bar{E} is used as variable instead of QF. The average specific dose equivalent values of the two subsets differ by about a factor of ten. The straight line represents the fit to a linear regression equation. As expected the fit is very good.

SLIDE #4

The variables of the previous two figures are evaluated quantities based on the derived differential energy spectra and the appropriate conversion factors. At this point we introduce the sphere responses, response ratios and the combinations of these with the evaluated quantities as new variables. In Figure 4 the logarithm of the ratios of the 10 in. and 3 in. sphere responses, R_{10}/R_3 , versus the quality factors, QF, are shown. The resulting graph is similar to the one in Figure 3 albeit the specific dose equivalent values are replaced with the response ratios of the 10 in. and 3 in. spheres, suggesting that the response ratios may take place of at least one of the derived quantities.

Again the separation of the reactor and calibration measurements is apparent. The line is linear regression fit to all the measurements, and using this linear fit the quality factors of the reactor measurements in half of the cases will be underestimated. The bare ^{252}Cf and Al - moderated ^{252}Cf fission sources show the largest deviation.

SLIDE #5

The quality factors and the logarithm of the sphere response ratios are interchangeable as shown in Figure 4, therefore next the behaviour of the specific dose equivalent as function of the different sphere response ratios were investigated. In Figure 5 the specific dose equivalent values versus the ratios of the 8 in. and 3 in. sphere responses, R_8/R_3 are shown on a log-log scale. The distinct separation of the reactor and calibration measurements is evident.

The dynamic range of the response ratios, which indicate how well this method could determine the specific dose equivalent, of all the measurements is 25 and of all the reactor measurements is 2.2, which is not quite a large range. Nevertheless these response ratios could be used to distinguish reactor measurements from calibration ones. We must emphasize when we talk about calibration measurements of the ones used in the present experiments are in that category.

SLIDE #6

The functional dependence of the specific dose equivalent values versus the ratio of 10 in. and 3 in. sphere responses, R_{10}/R_3 , plotted on a log-log scale are shown in Figure 5. This seems to be more linear than the previous plot. The dynamic range of the response ratios of all the measurements also increased to 80 and the reactor measurements to 7. This increment of dynamic ranges makes the R_{10}/R_3 ratios a better measure of the specific dose equivalent values than the R_8/R_3 ratios. The linearity of the plot increased, however the separation of the reactor and calibration source measurements is still evident.

FIGURE 7

In the present studies the quality factor (QF) was almost exclusively used in place of the average energy, \bar{E} , a well known and extensively used quantity in neutron spectroscopy. The functional dependence of the measured and evaluated quantities in terms of \bar{E} are under investigation and only one example of this ongoing study presented in Figure 7, where the \bar{E} versus ratio of 10 in. and 3 in. sphere responses, R_{10}/R_3 are shown on a semi-log scale (Note the break in the abscissa at 2.9). This figure illustrates a clear cut difference between the presently used calibration sources and reactor measurements. It also indicates that if the average energy calibration was based on bare ^{252}Cf , Al - and H_2O moderated fission spectra measurements then the average energy of a reactor spectrum can not be determined from sphere response ratio measurements. The average energy of a reactor neutron spectra can not be determined from the average energies and ratio of 10 in. and 3 in. sphere responses of calibration sources.

SLIDE #8

The term "rem meter" is quite familiar to any practitioner of health physics. Rem meters are usually single moderator and single detector instruments. Many attempts have been made in the past to design and build such instrument

for neutron dosimetric purposes from thermal to say 20 MeV energy range. Based on the present experiments an 8 in. "rad meter" was "constructed". In Figure 8 the ratio of the response of the 8 in. sphere, R_8 , and the measured absorbed dose rate values versus the quality factors are shown. The use of the quality factor separates the reactor and calibration source measurements into the now familiar two subsets. A bare ^{252}Cf fission source seems to be a good calibration source however the measured absorbed dose rate values would be ± 40 percent accurate.

SLIDE #9

Next the behaviour of simple "rem meters", based on the responses of the 8 and 12 in. spheres were investigated. The independent variable, the abscissa, is again the quality factor, and the ordinate the sphere responses R_8 and R_{12} , divided by the dose equivalent rate values. Calibrating with bare ^{252}Cf fission neutron sources the 8 in. "rem meter" will over-respond to stray neutrons of a PWR by as much as a factor of 5 and the 12 in. sphere will under-respond in most cases. Visual inspection of the 8 in. "rem meter" response suggests that there might be a quality factor dependent correction factor which possibly could flatten the response of this detector. The sensitivity of the 8 in. "rem meter" is good and 6 counts per minute corresponds to $4 \mu\text{rem/h}$.

SLIDE #10

A "rem meter" constructed from the 10 in. sphere has the flattest response. In Figure 10 the response of the 10 in. sphere divided by the dose equivalent values versus the quality factors are shown. A simple device, such as this may be usable for reactor measurements. If this instrument is calibrated with a bare ^{252}Cf source the dose equivalent rates might be overestimated by about a factor of 2. The sensitivity of this device is good, 6 counts per minute correspond to $10 \mu\text{rem/h}$. It may be possible to obtain a calibration factor from the data presented in Figure 4 ($\log R_{10}/R_3$ vs. QF) to make the response of this detector linear.

SLIDE #11

The measured dose rate of bare point sources of different source strength versus the total neutron flux in the same geometry are in constant proportion such as line a in Figure 11. However it came as some of a surprise that the reactor measurements, including the D_2O moderated ^{252}Cf fission source, are also in near constant proportion as shown in line b. Linear regression analyses indicate that the slope of the bare ^{252}Cf measurement

curve is 1, as it should be. The slope of the curve for the reactor measurements plus the D₂O calibration is 1.05 ± 0.03 . The correlation coefficients are over 0.99. The equation for the dose rate in rad/h in terms of the total flux, ϕ , in $n/(cm^2 s)$ is: dose rate (rad/h) = $1.9 \phi^{1.1}$.

SLIDE #12

Finally, the evaluated dose-equivalent rates versus the total flux values are shown in Figure 12. Note that the application of the quality factors separates the data into three distinct groups. One is the calibration measurements, line a, where the specific dose equivalent is greater than 2×10^{-8} ; the second group, line b, has specific dose equivalent ranging from 2×10^{-9} to 1×10^{-8} , and the third group line c, where the specific dose equivalent are less than 2×10^{-9} . The slope of the regression lines for each of the separate groups are very near to one, and the correlation coefficients are over 0.96.

The dose equivalent rates at the operating level of the reactors are in terms of the total neutron flux

$$\text{d.e. rate (rem/h)} = 14 \phi$$

and at the middle level of the reactor

$$\text{d.e. rate (rem/h)} = 4.7 \phi$$

5. CONCLUSION

We showed that the neutron differential energy spectra, average energy, quality factor and the dosimetric quantities of the stray neutron radiation fields in the containments of the PWR's can be determined using low resolution moderating sphere neutron spectrometers. The physical and dosimetric quantities are estimated to be accurate to within 10 to 15 percent.

Based on 31 measurements at six PWR's of somewhat different design, simple linear relations were found for the dose and dose-equivalent rates as a function of the total flux, ϕ . These indicate that in containments of PWR's the problem of dose equivalent rate determination might be reduced to the measurement of the total neutron flux.

REFERENCES

1. Rossi, H. H., Mays, C. W., Health Phys. 34 (1978) 353
2. Hankins, D. E., Griffith, R. V., "A Survey of Neutrons Inside the Containment of a Pressurized Water Reactor", in Radiation Streaming in Power Reactors, USDOE Rep. ORNL/RSIC-43 (1979) 114
3. Bricka, M., "Neutron Measurements Near PWR Power Reactors", in Seventh DOE Workshop on Personnel Neutron Dosimetry, USDOE Rep. PNL-2807 (1978) 103
4. Butler, M. H., Ohnesorge, W. F., Auxier, J. A., "Measured Distribution of Neutrons Inside Containment of a PWR", in Radiation Streaming in Power Reactors, USDOE Rep. ORNL/RSIC-43 (1979) 110
5. Hankins, D. E., A Modified-Sphere Neutron Detector, USDOE Rep. LA-3595 (1967)
6. McLaughlin, J. E., O'Brien, K., "Accelerator Stray-Neutron Dosimetry: Spectra of Low- and Intermediate-energy Neutrons", in Neutron Monitoring, IAEA, Vienna (1967) 335
7. Sanna, R. S., "Modification of an Iterative Code for Unfolding Neutron Spectra from Multisphere Data", USDOE Rep. HASL-311 (1976)
8. Casson, R. M., Benton, E. V. "Nuclear Track Detection", 2 (1978) 173

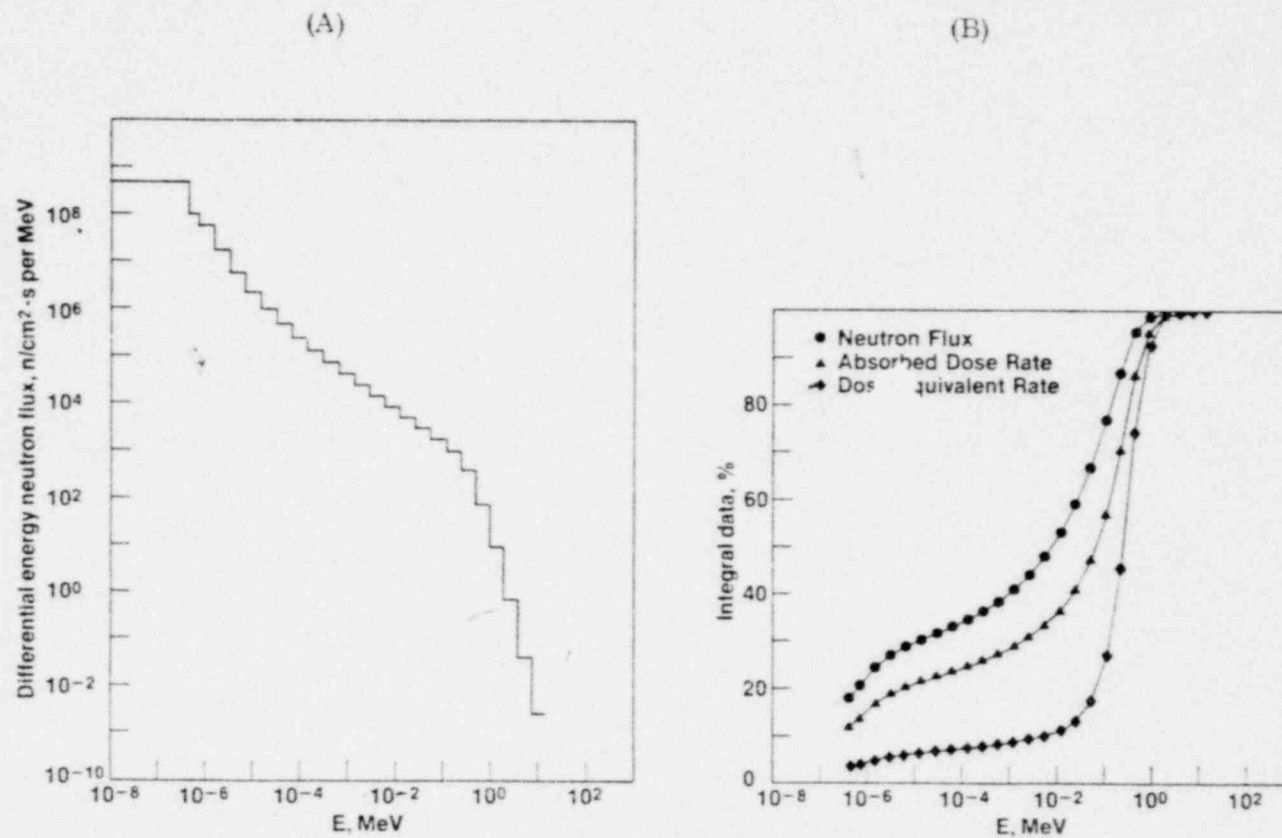


Figure 1. Differential neutron energy spectra measured in the vicinity of the pressure vessel of a PWR on the operating floor: a) differential energy spectra; b) cumulative percentage of neutron flux, absorbed dose and dose-equivalent rates versus the neutron energy.

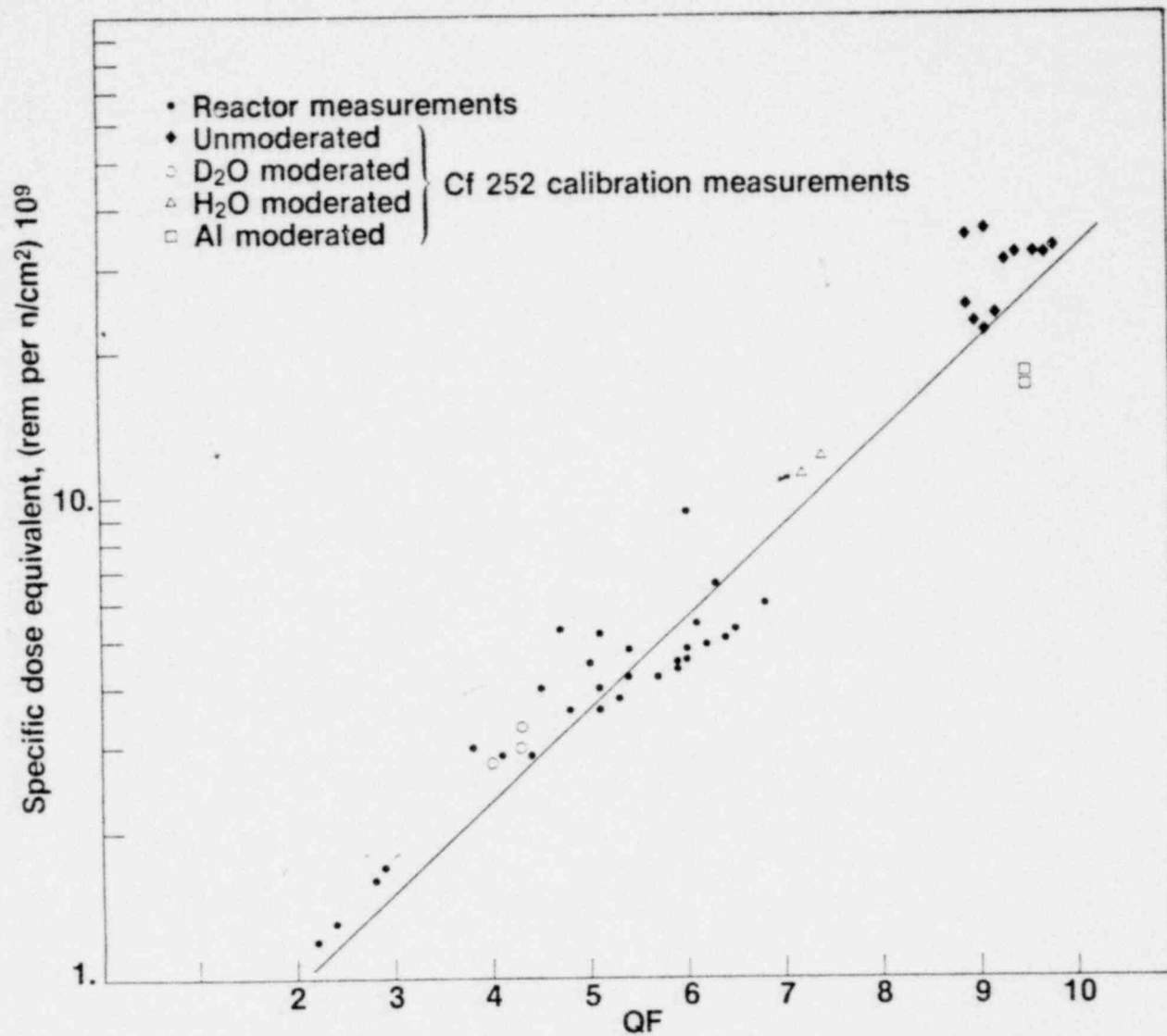


Figure 3. The specific dose-equivalent values versus the quality factors, QF. The solid line is the linear regression curve.

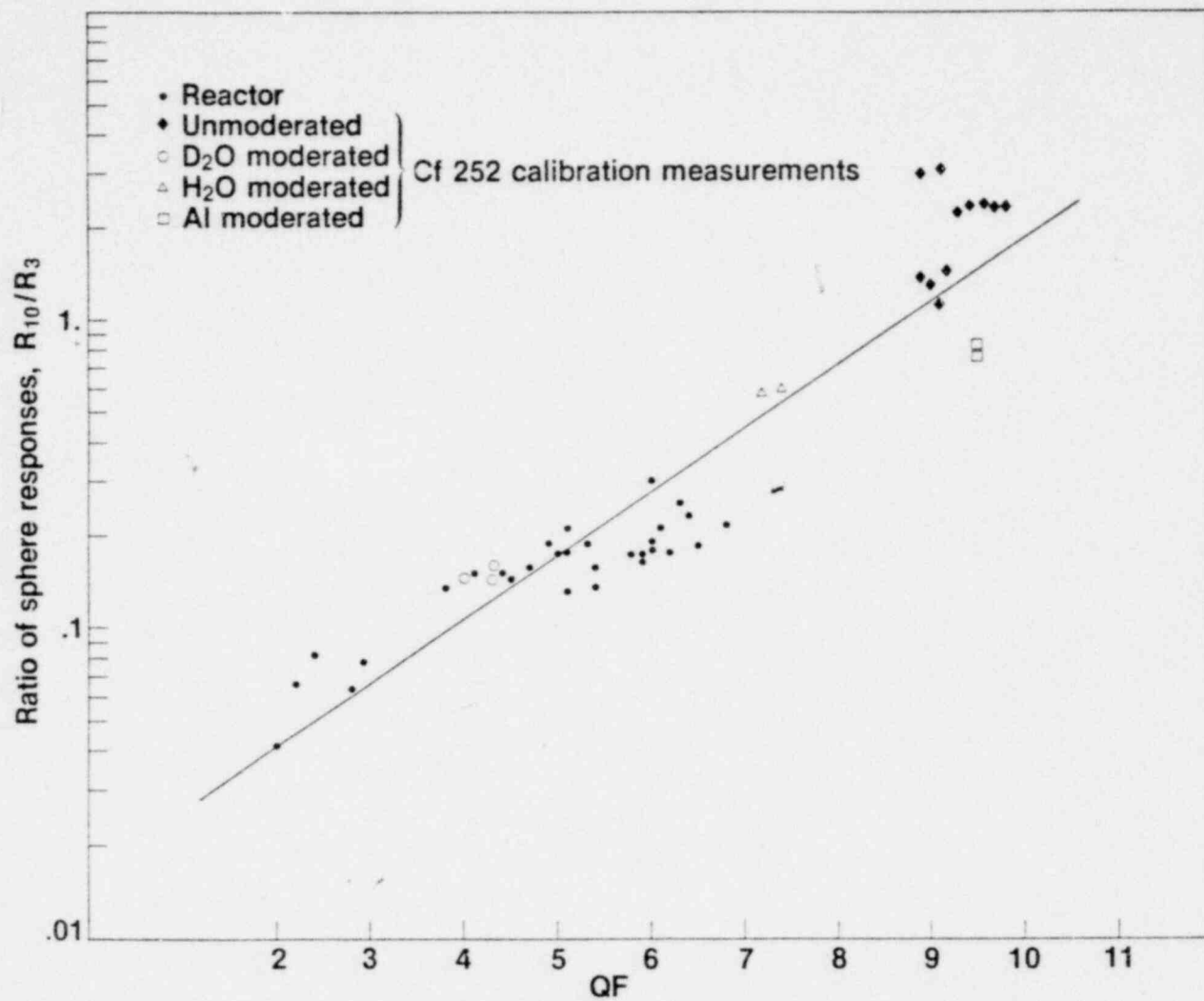


Figure 4. The ratios of 10 in. and 3 in. sphere responses, R_{10}/R_3 , versus the quality factor, QF. The solid line is the linear regression curve.

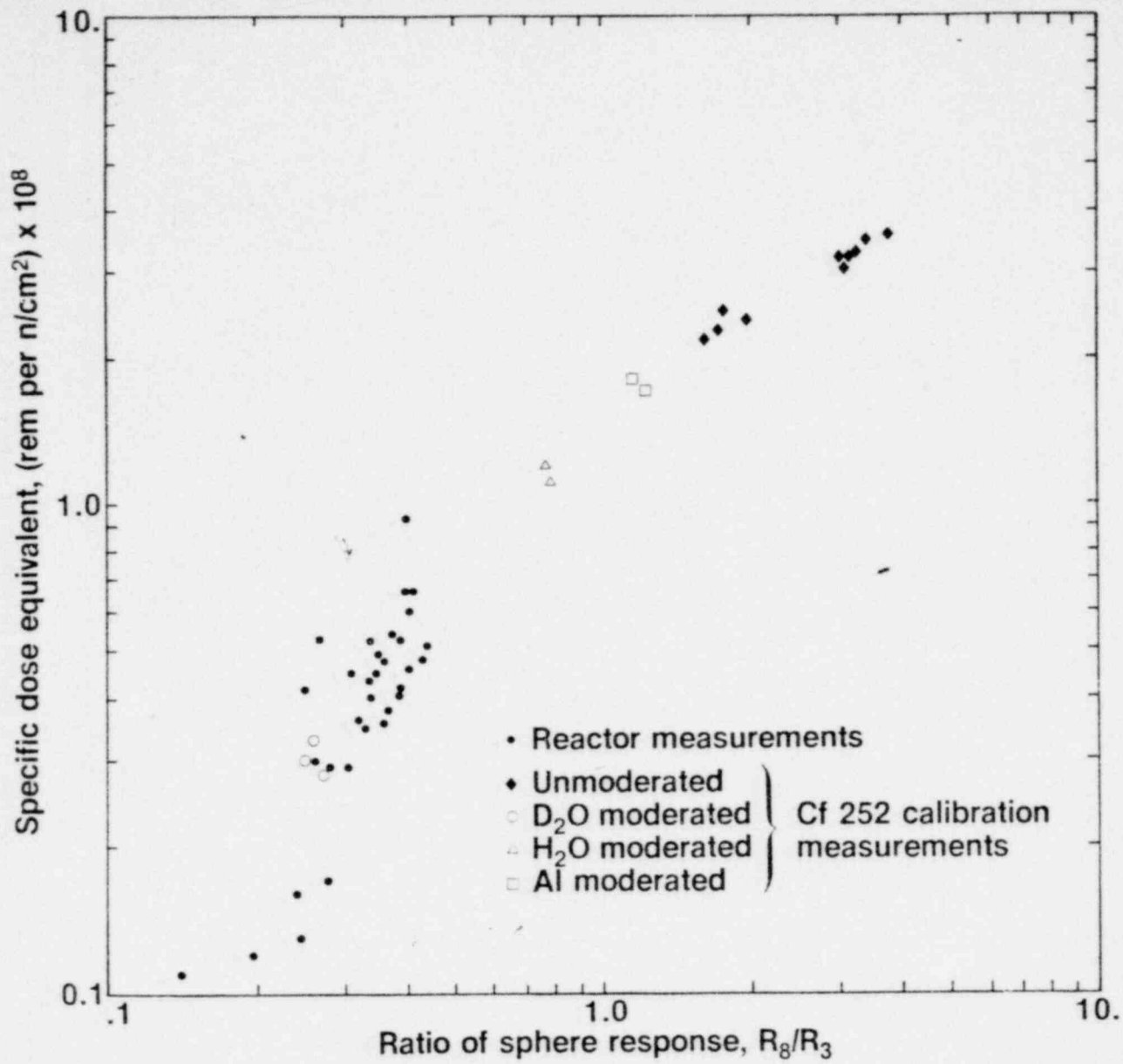


Figure 5. Evaluated specific dose equivalent, rem per n/cm² x 10⁸, versus ratio of 8 in. and 3 in. sphere responses, R_8/R_3 .

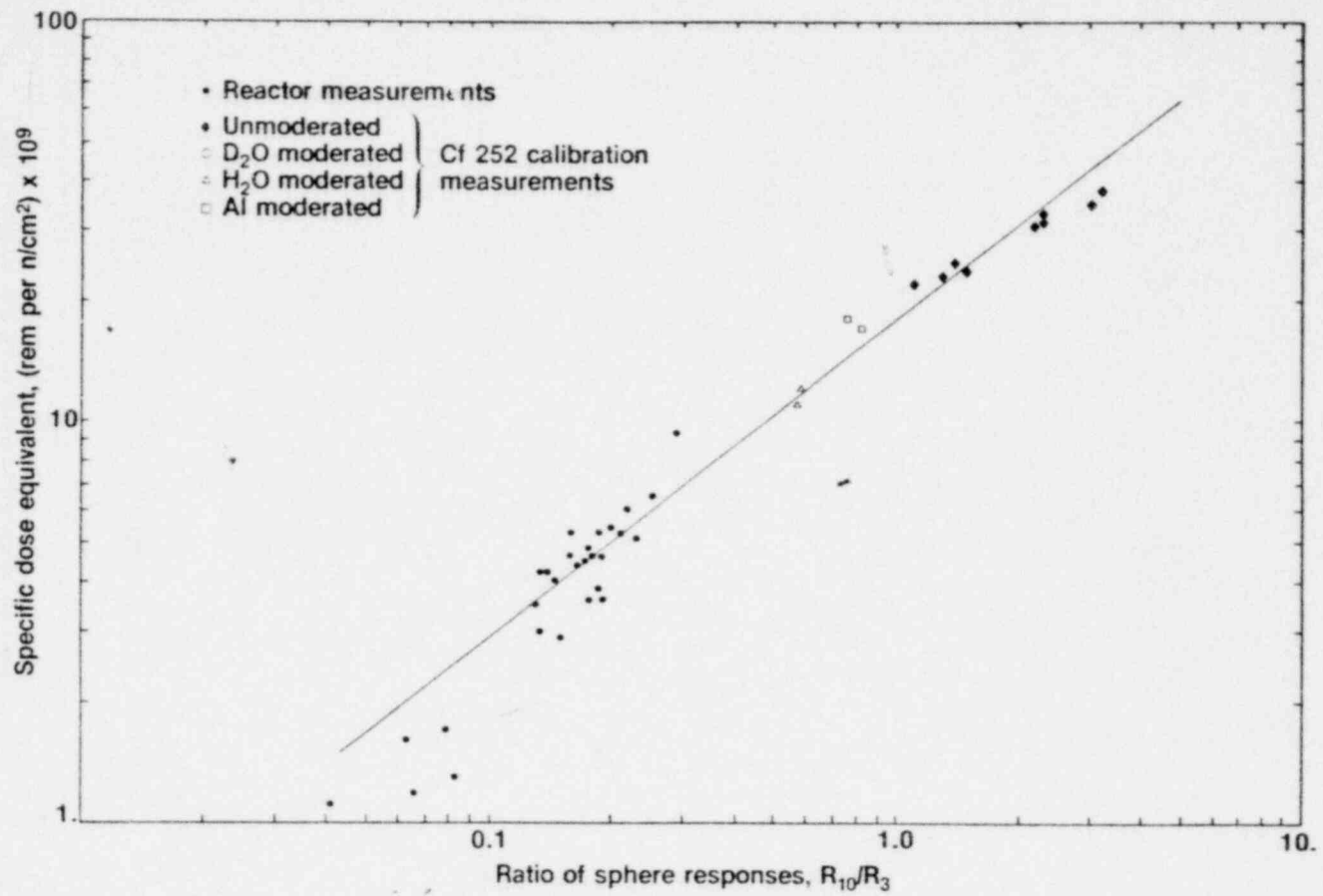


Figure 6. Evaluated specific dose equivalent, rem per n/cm² x 10⁹, versus ratio of 10 in. and 3 in. sphere responses, R₁₀/R₃. The solid line is the linear regression curve.

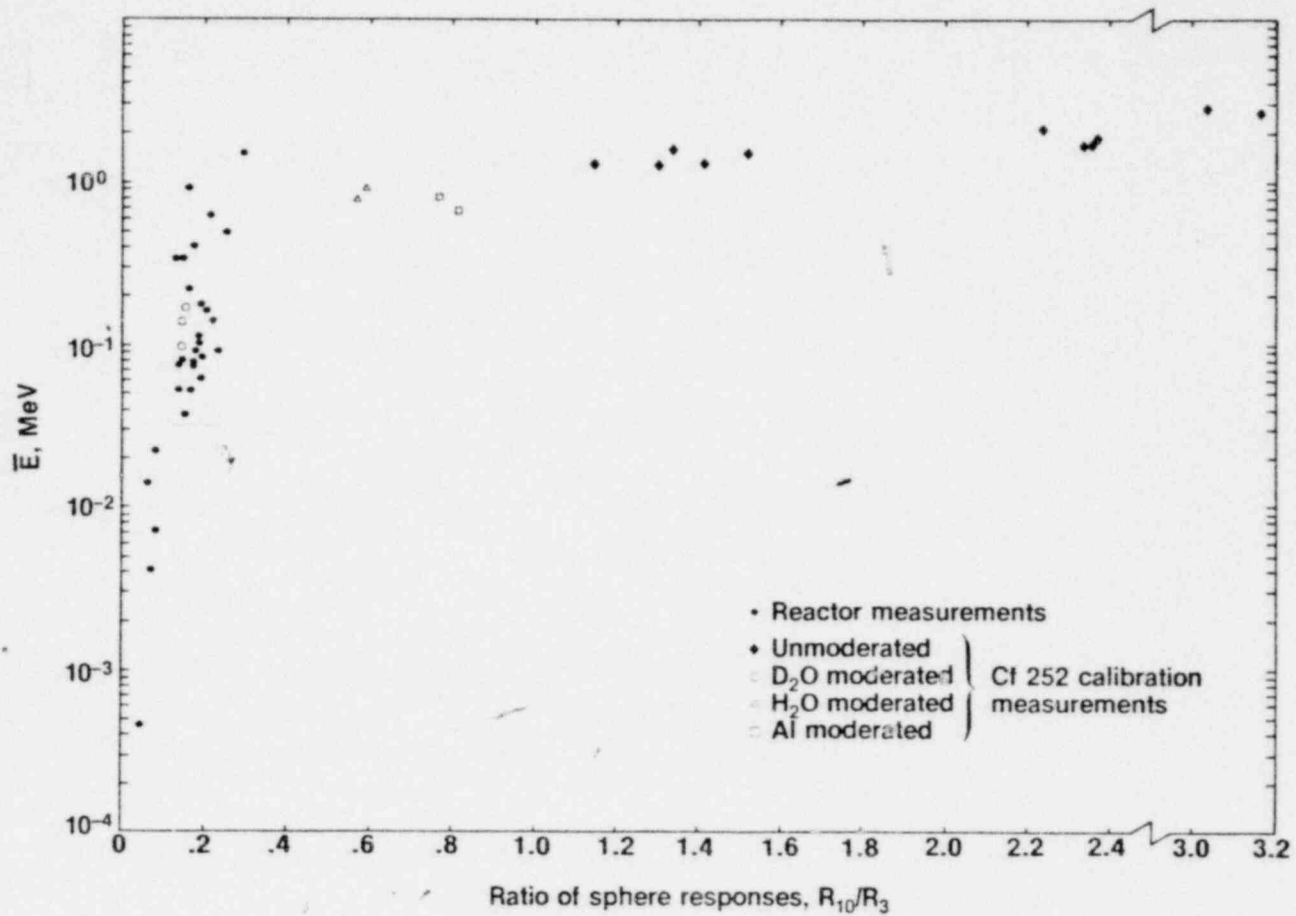


Figure 7. Evaluated average energy, \bar{E} (MeV) values versus the ratio of 10 in. and 3 in. sphere responses. Note the discontinuity in the abscissa after $R_{10}/R_3 = 2.4$.

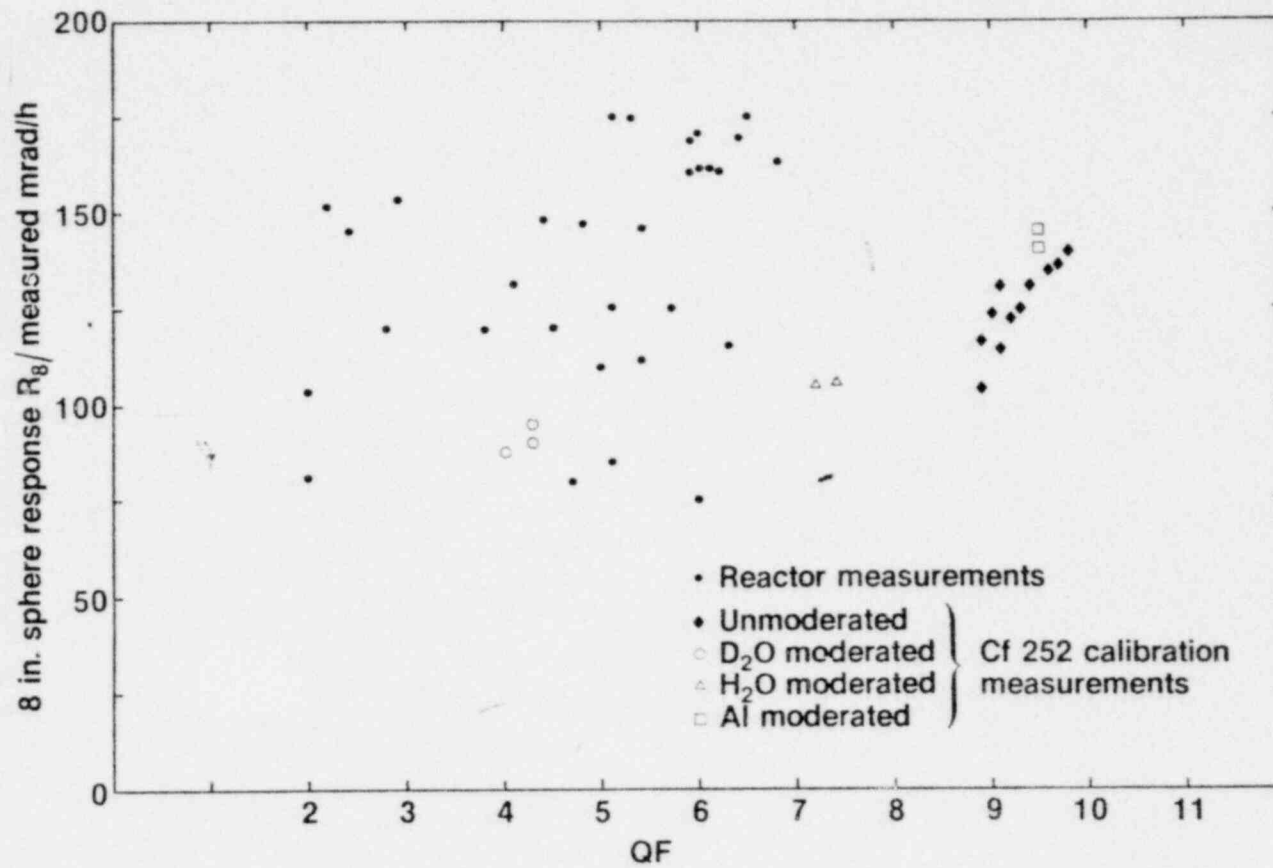


Figure 8. The evaluation of a "rad meter" : The response of the 8 in. sphere divided by the measured dose rate, mrad/h, versus the quality factor, QF.

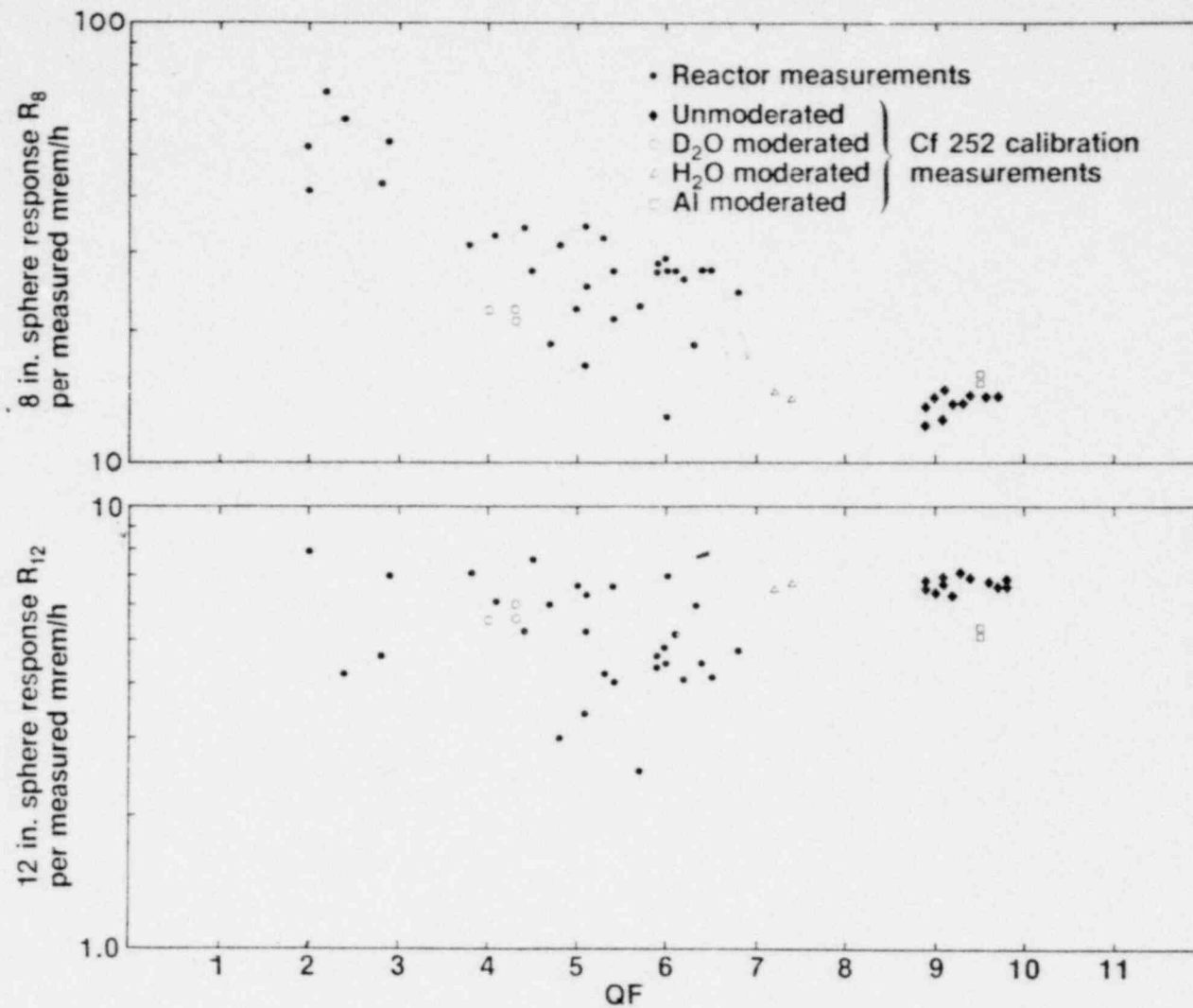


Figure 9. The evaluation of two "rem meters";
 Upper diagram: the response of an 8 in. sphere,
 Lower diagram: the response of a 12 in. sphere,
 each of them divided by the measured dose equivalent
 rate, mrem/h, versus the quality factor, QF.

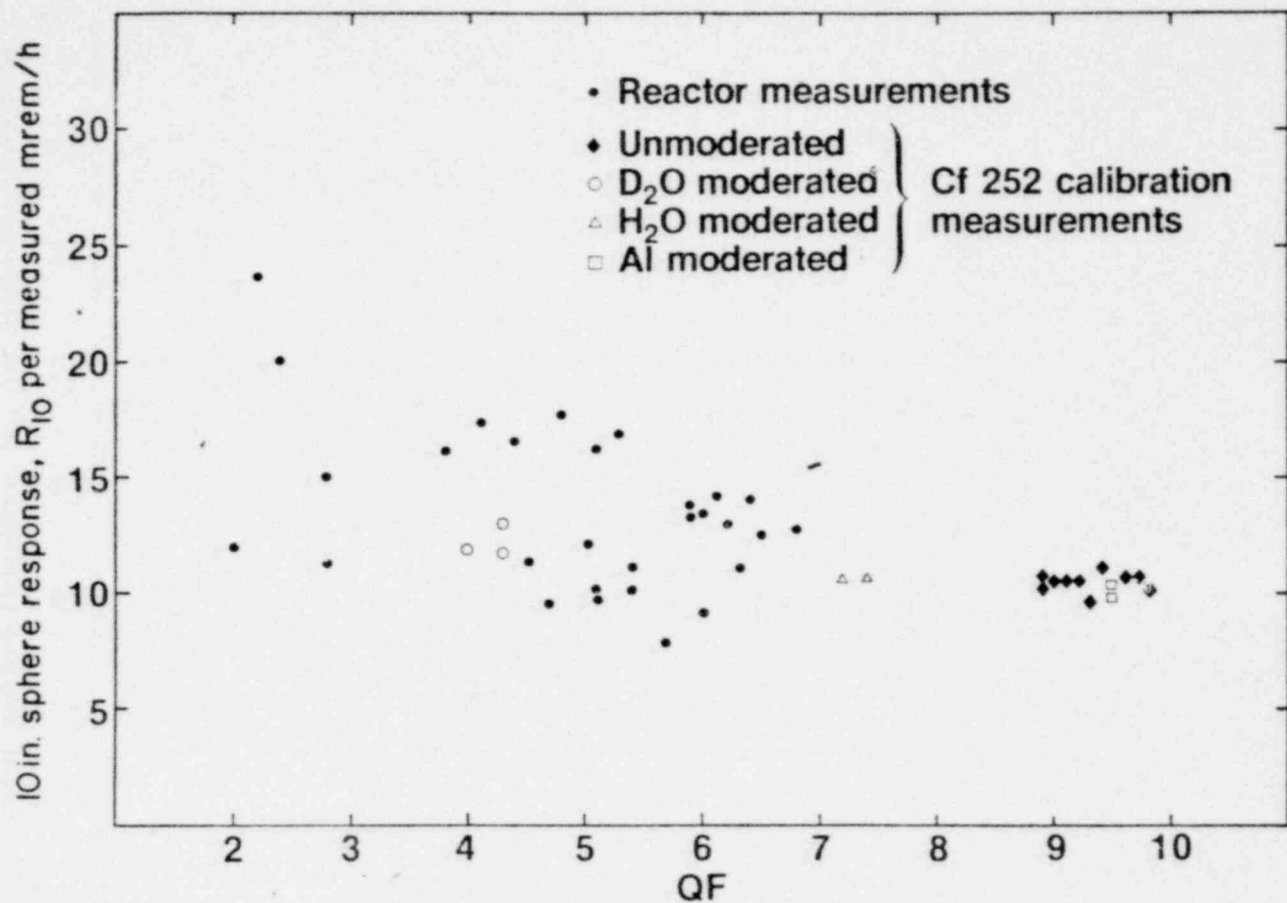


Figure 10. The evaluation of a 10 in. spherical "rem meter"; The response of a 10 in. sphere divided by the measured dose equivalent rate, mrem/h, versus the quality factor, QF.

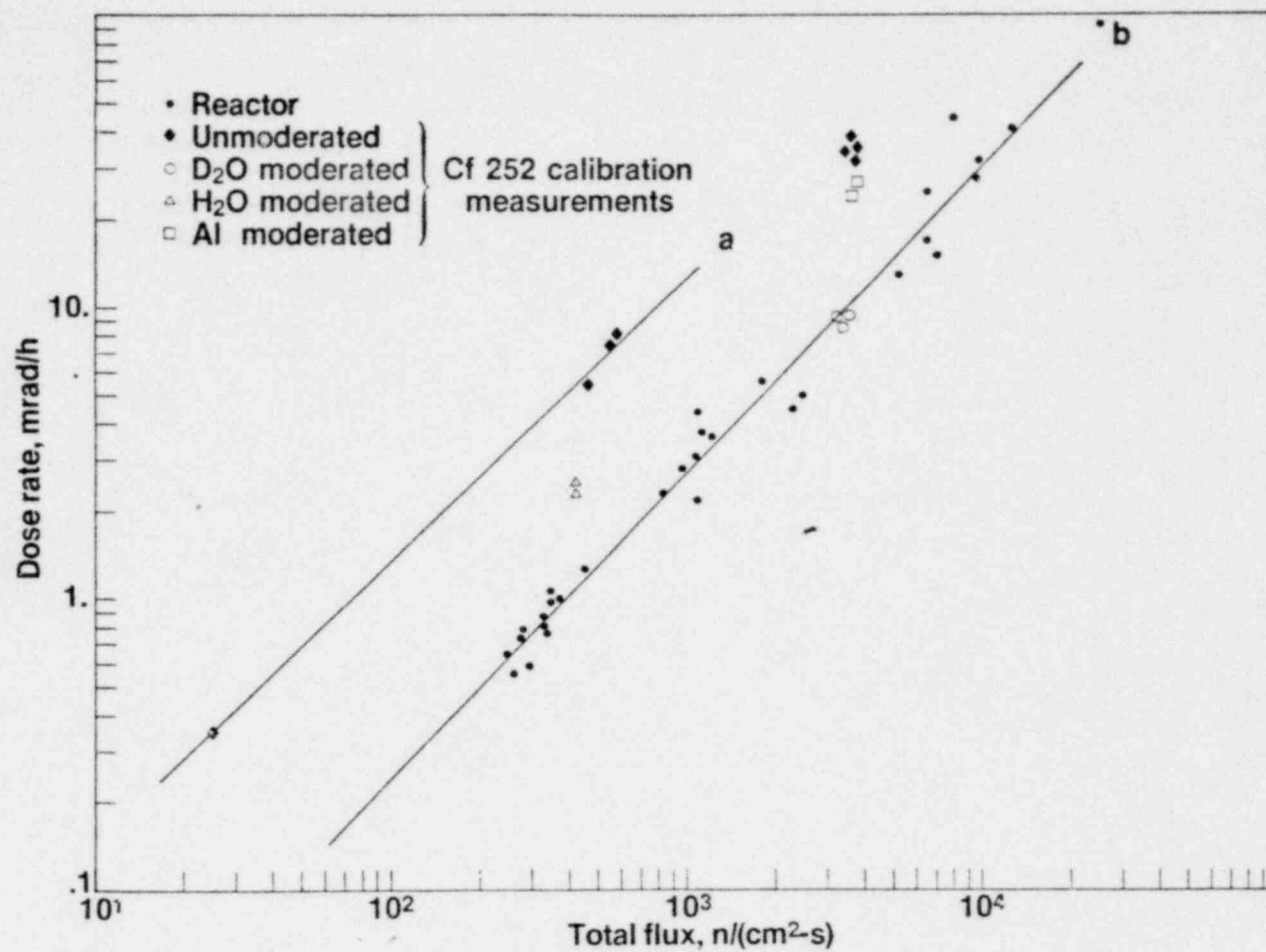


Figure 11. Dose rate versus the total flux of neutrons: line a - from unmoderated ²⁵²Cf fission sources, line b - in the containments of the reactors plus D₂O-moderated fission source.

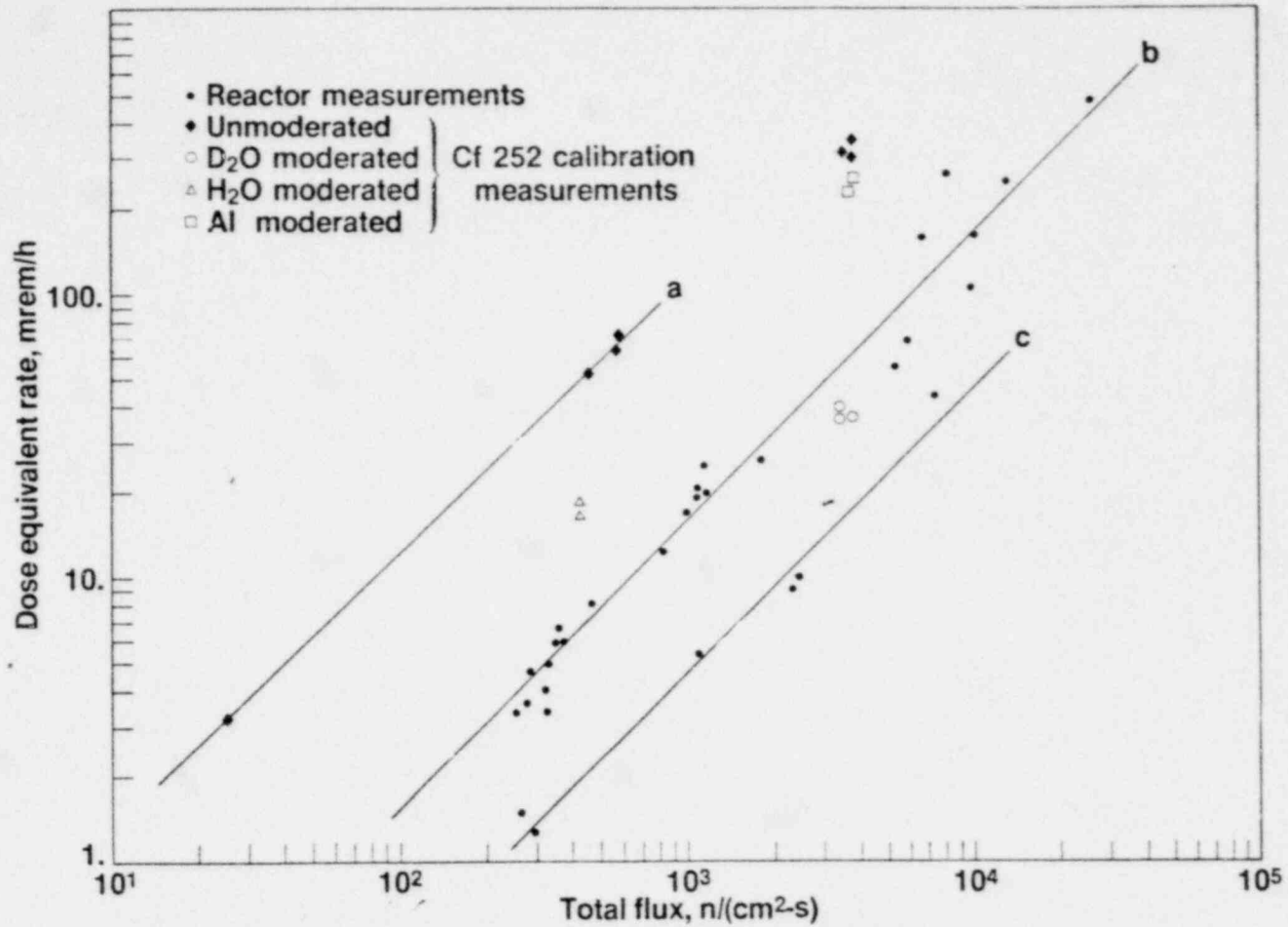


Figure 12. Dose-equivalent rate versus the total flux of unmoderated ²⁵²Cf fission sources, line a; the reactor measurements on the operating floor level plus the D₂O moderated fission source, line b; and the reactor measurements on the medium floor level, line c.



INTERNATIONAL ATOMIC ENERGY AGENCY
OECD NUCLEAR ENERGY AGENCY



INTERNATIONAL SYMPOSIUM ON OCCUPATIONAL RADIATION EXPOSURE IN NUCLEAR FUEL CYCLE FACILITIES

Los Angeles, USA, 18-22 June 1979

IAEA-SM-242/ 24

STRAY NEUTRON FIELDS IN THE CONTAINMENT OF PWRs

Ferenc Hajnal and Robert S. Sanna

Environmental Measurements Laboratory
U. S. Department of Energy
New York, NY 10014

Robert M. Ryan and Elizabeth H. Donnelly

Rensselaer Polytechnic Institute
Troy, NY

POOR ORIGINAL

This is a preprint of a paper intended for presentation at a scientific meeting. Because of the provisional nature of its content and since changes of substance or detail may have to be made before publication, the preprint is made available on the understanding that it will not be cited in the literature or in any way be reproduced in its present form. The views expressed and the statements made remain the responsibility of the named author(s); the views do not necessarily reflect those of the government of the designating Member State(s) or of the designating organization(s). *In particular, neither the IAEA nor any other organization or body sponsoring this meeting can be held responsible for any material reproduced in this preprint.*

STRAY NEUTRON FIELDS IN THE CONTAINMENT OF PWRs

ABSTRACT

Multisphere neutron spectral measurements were performed at six pressurized water reactors (PWRs). The measured differential neutron energy spectra and flux were used to determine average energy, quality factor, dose and dose-equivalent rates. The maximum quality factor found was 7. The neutron spectra varied from a highly moderated one with $\bar{E} = 1$ keV to a less moderated one with $\bar{E} = 0.7$ MeV. Simple linear relations were found to calculate the dose and dose-equivalent rates from the total neutron flux. The dose-equivalent rates on the operating floor level are fourteen times and on the middle level five times the total neutron flux.

1. INTRODUCTION

There have been few systematic investigations of the stray penetrating radiation fields to which workers and instruments are exposed inside the containments of nuclear power reactors. The recent concern about neutron exposure in these mixed fields inside pressurized water reactor containments and how adequately neutrons are routinely monitored has apparently motivated the development of data needed to evaluate the distribution of doses to workers and to determine acceptable levels of exposure [1].

Gamma radiation monitoring of operations and maintenance staff is performed relatively easily. The determination of neutron dose or dose-equivalent values and their distributions with neutron energy in the presence of significant gamma-ray levels inside and near PWR containments with available instrumentation is more difficult. The unpleasant if not hostile conditions of high ambient temperature and humidity and possible airborne and surface radionuclide contamination are barriers to the required spectrometric investigations.

Recently, measurements have been made with various devices, such as low energy resolution, moderating sphere systems and with fission counters using ^{235}U , ^{238}U and ^{237}Np in conjunction with various thermal neutron absorbers [2,3]. Polycarbonate track etch detectors with ^{238}U , ^{237}Np and ^{239}Pu fission foils also have been used to measure neutron flux and to obtain dose-equivalent rates [4]. While neutron spectra can be found by unfolding the multisphere and fission counter data, the track etch system provides approximate spectral information that is only sufficient to set an upper limit on the applicable quality factors. Properly calibrated neutron survey meters supplement such spectral measurements to obtain rapid estimates of neutron dose-equivalent rates [2]. One type of survey instrument is equipped with both 3 and 9 in. diameter moderator spheres and the sphere response ratio is also used as an indicator of the spectral shape and to interpret personnel neutron dosimeter readings [5].

The present paper reports some results of a collaborative study performed in the containments of six PWRs of somewhat different design and construction. Both passive LiF thermoluminescence detectors (TLD) and active LiI(Eu) scintillators were employed as thermal neutron detectors with the multisphere systems. Dosimetric quantities, such as absorbed dose and dose equivalent, as well as values of average energy, \bar{E} , for the neutron field and the quality factor, QF, were obtained from the spectral determinations. Tentatively, the results indicate that rapid estimates of quality factors and average energies may be obtained, as Hankins has indicated [5], from the ratios of measurements performed with different moderator spheres.

2. THE MULTISPHERE NEUTRON SPECTROMETER SYSTEM

The multisphere system was adapted from a system used in previous studies around particle accelerators [6]. Six different diameter (2, 3, 5, 8, 10 and 12 in.) polyethylene moderating spheres along with a bare neutron detector and one covered with a 0.032 in. thick cadmium absorber form the system. The neutron detectors are paired ^6LiF and ^7LiF TLDs, and 4×4 mm and 12.7×12.7 mm cylindrical $^6\text{LiI(Eu)}$ scintillators. The energy response functions of the detectors were calculated in 26 evenly spaced logarithmic intervals from thermal to 26 MeV. Due to the wide energy bins, resonance effects are smoother and there is no line structure in the response function. It is unlikely that any fine structure can be observed in the spectra. Higher resolution spectrometers are needed to resolve resonance scattering and absorption peaks, such as those at 25 and 28 keV, produced by selective filtering in the iron of the reactor pressure vessel [7].

Each thermoluminescence detector has four each of ^6LiF and ^7LiF chips stacked to form two separate $3.2 \times 3.2 \times 3.6$ mm columns, whose surface areas are the same as that of the equivalent sphere used in the calculations of the 4×4 mm right cylindrical scintillator response function. The 4×4 mm ^6Li responses, after normalization, were used in unfolding both types of spectrometric measurements [8]. Resonance scattering and absorption by the fluoride were neglected. The net signal due to the $^6\text{Li}(n, \alpha)$ reactions are extracted from the TLD measurements after individual chip responses are corrected for observed loss of sensitivity due to neutron irradiation damage. The TLD stacks were positioned inside the cadmium covers in the same geometry to minimize readout differences due to the neutron capture gamma radiation from the cadmium.

The use of highly enriched LiI(Eu) results in good resolution (about 9 percent) and in high light output which makes gamma-ray background differentiation relatively easy and reliable. In practice, the measurements are recorded on a multichannel analyser and the background as represented by the area remaining after a straight line background under the neutron peak is subtracted.

The measurements were unfolded with a modified version of the BON code, an iterative unfolding method that successively corrects trial solutions finding only non-negative values, while the deviation between the measured and computed detector responses is minimized. The process is usually terminated after 1000 iterations [8]. It is inherent of iterative least-squares unfolding techniques that sometimes only a reasonably smooth unfolded spectrum can be obtained from measurements with poor statistics. Care must be taken to assure that the measurement is good before the unfolded spectrum is accepted. Tests are

being made to resolve this problem, but reliance on inter-laboratory comparison measurements is necessary at present.

3. REACTOR MEASUREMENT METHODS

The scintillation detectors performed very well in gamma-ray fields up to tens of mrad/h combined with neutron contributions of tens of mrem/h. The 4 X 4 mm scintillator was more useful for higher neutron dose rates and the 12.7 X 12.7 mm scintillator for higher gamma-ray dose rates.

Both spectrometer systems were calibrated with bare and D₂O-, H₂O- and aluminum-moderated ²⁵²Cf fission sources. The calibration factors obtained with three different bare sources agreed to within ±4 percent.

The measurements in the containments of the PWRs were usually made at one meter from the floor level. Data were acquired by switching moderator spheres between the two scintillators, and the acquisition of the complete data set of two spectra required about 30 minutes. Data acquisition with the TLD system required a minimum of several hours, while in low neutron fields, the TLD system was exposed for two or three days.

Data from the active system were accumulated with a multi-channel analyzer and stored on magnetic tape for later analysis. Due to high ambient temperature and humidity in the containment, the electronics were enclosed in an insulated, air tight container cooled with dry ice and dried with silica gel. The dry ice kept the inside temperature below about 40°C for two days, and the closed container protected the instrumentation from contamination.

The reactor pressure vessel, in the center of the containment, rests on the vessel support structure and is surrounded by the primary shield. The reactor vessel support structure rests on the lowest elevation of the containment. Above this, there are two or three more floors that are accessible to personnel. The radiation levels at different floors will vary according to the power level of the reactor and the shielding design and construction.

The neutrons from the core encounter different amounts of shielding due to the exact design. There may be additional shielding on the top of the reactor. In case of older PWRs, neutron streaming is not of major importance. In newer designs, to reduce the possible high asymmetric pressure load on the reactor vessel and biological shield which could result from a major malfunction, the upper part of the region was enlarged and resulted in an increased neutron and gamma-ray streaming.

On the lowest and medium containment levels, gamma radiation usually dominates, and on the top or operating level, neutrons are dominant. The radiation levels may vary from a

few mrem/h to many rem/h, therefore, a detailed area survey is necessary prior to neutron measurements. Most of the present measurements were performed on the top levels where radiation fields often have large spatial gradients. Also surveyed were important areas where personnel and equipment are transferred into the containment through an airlock or hatchway.

4. RESULTS AND DISCUSSION

The energy spectra derived by unfolding the multisphere measurements were used to calculate the integral quantities, such as neutron flux, average energy (\bar{E}), absorbed dose and dose-equivalent rate and quality factor (QF). An example of the differential energy spectra, measured on the operating floor near the reactor cavity and the control drive mechanism is shown in Figure 1. This neutron spectrum is relatively "hard"; \bar{E} is 90 keV and the quality factor is 6.4. The absorbed dose rate is 3 mrad/h, the dose-equivalent rate is 19 mrem/h, and the total neutron flux is $1060 \text{ n/cm}^2 \text{ s}$. Eighteen percent of the neutrons are thermal and about 13 percent have energies greater than 300 keV, that is over the threshold energy of the track etch detectors [9]. Generally, the differential energy spectra have thermal groups of various intensities followed by an approximately $1/E$ distribution. Then, depending on the \bar{E} and QF, the spectra may decline rapidly. In the case of $\bar{E} = 7 \text{ keV}$, for example, a rapid decline sets in at about 40 keV and virtually no neutrons are found over 200 keV.

The 31 spectral measurements have a wide range of \bar{E} , from 0.1 keV to about 1 MeV, with the \bar{E} of 26 of these measurements being from 10 keV to 1 MeV. The quality factor distribution showed two peaks; 24 were from 4 to 7 and 6 from 2 to 3. The summary of \bar{E} and QF is in Table I. There seems to be no simple \bar{E} versus QF dependence.

Larger quality factors were dominant on the top or operating floor and somewhat small values, $QF < 3$, for the middle levels of the reactors. For the very large \bar{E} change, from 0.1 to 100 keV, the quality factor changes only from 2 to 4. For the 24 measurements which have QF equal to 4-7, \bar{E} changes only from 40 keV to 1 MeV. The single $\bar{E} > 1 \text{ MeV}$ measurement point has a spurious peak in the unfolded spectrum at about 10 MeV, which might be attributed to the limitation of the unfolding procedure. The neutron flux varies moderately, from 2.5×10^2 to $2.6 \times 10^4 \text{ n/(cm}^2 \text{ s)}$, for all measurements which were performed evenly over this flux range. No unusually high thermal or fast flux fields were encountered. The frequency distribution of the neutron flux is shown in Table II.

The average energies can only be determined with lesser accuracy. The 10 and 3 in. sphere response ratios correlate very weakly with \bar{E} , having a correlation coefficient of only

0.2. Better results can be obtained by using the 8 and 3 in. response ratios to obtain $\bar{E} = 7.9 \times 10^{-3}$ (R_8/R_3) with an 0.5 correlation coefficient.

A hypothetical "rem" counter was constructed from the responses for the 10 in. sphere divided by the evaluated dose-equivalent rates versus the quality factors. The smallest ratios were for the ^{252}Cf calibration sources. A simple device like this is usable for reactor measurements, but if it is calibrated with a bare ^{252}Cf source most of the dose-equivalent rates will be overestimated by a factor of up to 2 [5]. A device constructed from the 8 in. sphere will over-respond by as much as a factor of 5 and the 12 in. sphere will under-respond by as much as a factor of 3.

Since the slope of the specific dose versus \bar{E} curve is small, 0.18, it is not quite unexpected that the evaluated dose rate versus the total neutron flux gives essentially a straight line, as shown in Figure 4. Linear regression analyses indicate that the slope of the bare ^{252}Cf measurements curve is 1, as it should be. The slope of the curve for the reactor measurements plus the D_2O calibration is 1.05 ± 0.03 . All correlation coefficients are close to one.

Finally, the evaluated dose-equivalent rate versus the total neutron flux curves are shown in Figure 5. Note that the application of the quality factors separates the data into three distinct groups. One is the calibration measurements where the specific dose equivalent is greater than 2×10^{-8} ; the second group has specific dose equivalent ranging from 2×10^{-9} to 1×10^{-8} , and the third group where the specific dose equivalent are less than 2×10^{-9} . The slope of the regression lines for each of the separate groups are very near to one, and the correlation coefficients are over 0.96.

To identify possible simple relationships, linear regression analyses were performed on the measured quantities, the detector responses and response ratios, and the evaluated quantities such as the flux and dose rate. For example, by plotting the specific absorbed dose against the average energy, on a log-log scale, the correlation analyses indicate that the reactor data plus the D_2O moderated ^{252}Cf measurements fit a line with a small slope and the bare ^{252}Cf , H_2O and aluminum-moderated ^{252}Cf measurements fit a line which has a much larger slope. Because the slope of the linear regression of the reactor data is small, the dependence on \bar{E} is weak. An example of good correlation between the specific dose equivalent and quality factor is shown in Figure 2. The specific dose equivalent in $\text{rem}/(\text{n}/\text{cm}^2)$ in terms of the evaluated quality factors, QF, is equal to $4 \times 10^{-10} \times (\text{QF})^{0.19}$, and the correlation coefficient is 0.96.

As expected, the quality factor, average energy, dose or dose equivalent per neutron per cm^2 are not measurable directly with a single instrument. Correlation analyses show that the

ratios of the responses of different sizes of detectors may provide an indirect method to determine these values. The quality factors may be determined from the response ratios of the 10 and 3 in. sphere data. Figure 3 shows these response ratios versus the quality factor. The quality factor, QF, may be calculated from the linear regression equation in terms of the response ratios of the 10 and 3 in. diameter spheres, R_{10}/R_3 , and the equation is $QF = 8.63 + 4.72 \log (R_{10}/R_3)$. The correlation coefficient is 0.92. Similarly one may obtain the specific dose equivalent from $\text{rem}/(n/\text{cm}^2) = 1.9 \times 10^{-10} (R_{10}/R_3)^{0.81}$, and the correlation coefficient is 0.97.

5. CONCLUSIONS

Since the operation of most of the instruments and the equipment of a PWR are monitored from the console, no routine in-containment inspections and surveys are necessary. Entry may be required in case of equipment failure, such as the breakdown of pumps or valves. Occasional in-containment checks of pressure and temperature gauges might be necessary. Extended area surveys, gamma and neutron, are usually performed in preparation for outages before major repair or refueling.

To verify the "rem" survey meter measurements at selected sites, the neutron differential energy spectra, average energy, quality factor and the dosimetric quantities of the stray neutron radiation fields in the containments of the PWRs can be determined using low resolution moderating sphere neutron spectrometers. The physical and dosimetric quantities are estimated to be accurate to within 10 to 15 percent. Simple relationships amongst the measured and evaluated quantities can be obtained using linear regression analysis.

Based on 31 measurements at six PWRs of somewhat different design, simple linear relations were found for the dose and dose-equivalent rates as a function of the total flux, ϕ , in $n/(\text{cm}^2 \text{ s})$. The equation is

$$\text{dose rate (rad/h)} = 1.9 \phi^{1.1}.$$

Similarly the dose-equivalent rate at the middle level of the reactor is

$$\text{d. e. rate (rem/h)} = 4.7 \phi$$

and at the operating level

$$\text{d. e. rate (rem/h)} = 14 \phi.$$

Since these equations are the result of all the measurements, good and bad statistics, the dose and dose-equivalent rates in some cases might be off by a factor of two. The equations simply

state that there are one-to-one relationships between the total neutron flux dose rates and the dose-equivalent rates.

ACKNOWLEDGMENTS

Special thanks are extended to J. E. McLaughlin who assisted in the measurements and in the preparation of this paper. We would also like to give out thanks to John Gulbin who did the TLD measurements, to Michael Boyle who provided excellent technical support, and to Edward Arrington who performed some of the computer programming, processed the large quantity of data and prepared the illustrations. We are also grateful to the management and technical staff of the six PWRs we visited for their assistance in performing these measurements.

REFERENCES

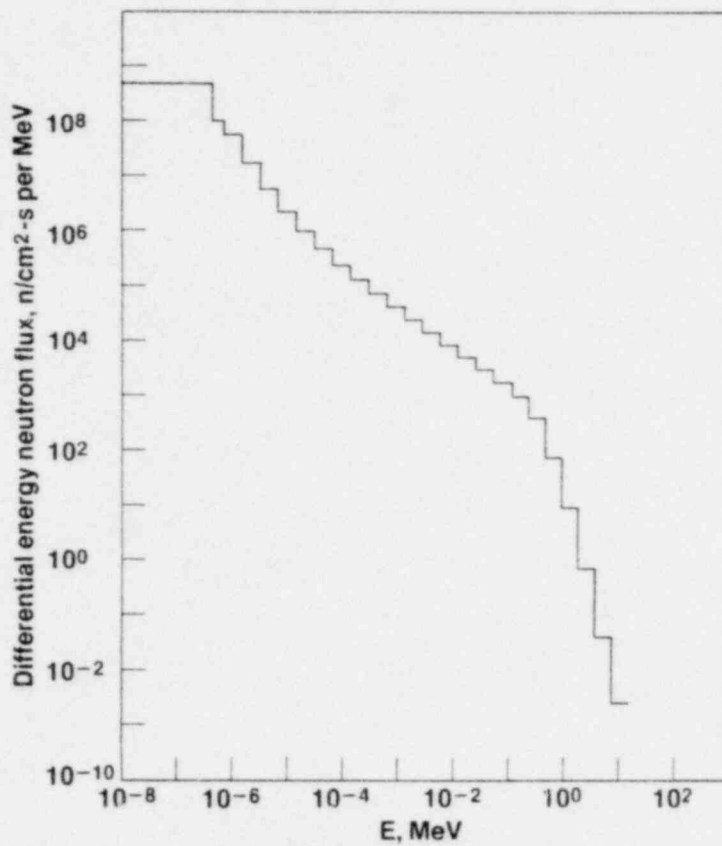
- [1] ROSSI, H. H., MAYS, C. W., Health Phys. 34 (1978) 353.
- [2] HANKINS, D. E., GRIFFITH, R. V., "A survey of neutrons inside the containment of a pressurized water reactor", in Radiation Streaming in Power Reactors, USDOE Rep. ORNL/RSIC-43 (1979) 114.
- [3] BRICKA, M., "Neutron measurements near PWR power reactors", in Seventh DOE Workshop on Personnel Neutron Dosimetry, USDOE Rep. PNL-2807 (1978) 103.
- [4] BUTLER, M. H., OHNESORGE, W. F., AUCIER, F. A., "Measured distribution of neutrons inside containment of a PWR", in Radiation Streaming in Power Reactors, USDOE Rep. ORNL/RSIC-43 (1979) 110.
- [5] HANKINS, D. E., A Modified-Sphere Neutron Detector, USDOE Rep. LA-3595 (1967).
- [6] McLAUGHLIN, J. E., O'BRIEN, K., "Accelerator stray-neutron dosimetry: spectra of low- and intermediate-energy neutrons," in Neutron Monitoring, IAEA, Vienna (1967) 335.
- [7] BENNETT, E. F., YULE, T. J., Techniques and Analyses of Fast-Reactor Spectroscopy with Proton Recoil Proportional Counters', USAEC Rep. ANL-7763 (1971).
- [8] SANNA, F. S., Modification of an Iterative Code for Unfolding Neutron Spectra from Multisphere Data, USDOE Rep. HASL-311 (1976).
- [9] CASSON, R. M., BENTON, E. V. Nuclear Track Detection, 2 (1978) 173.

TABLE I. DISTRIBUTIONS OF AVERAGE ENERGY, \bar{E} , AND OF QUALITY FACTOR, QF, FROM PWR NEUTRON MEASUREMENTS

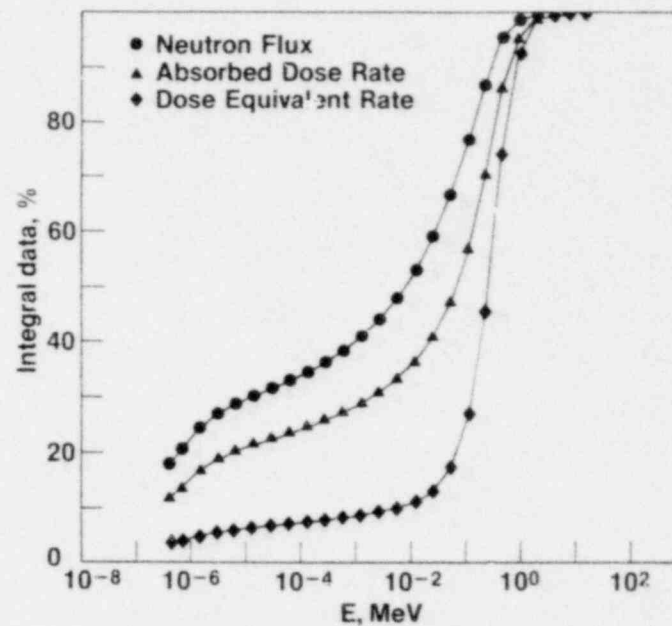
\bar{E} (MeV)	Frequency	QF	Frequency
$1 < \bar{E}$	1	6 - 7	9
0.1 - 1.0	13	5 - 6	10
$10^{-2} - 10^{-1}$	13	4 - 5	5
$10^{-3} - 10^{-2}$	2	3 - 4	1
$10^{-4} - 10^{-3}$	2	2 - 3	6

TABLE II. FREQUENCY DISTRIBUTION OF NEUTRON FLUX ($n/cm^2 s$)
FROM NEUTRON MEASUREMENTS SHOWN IN TABLE I

Energy	Flux			
	$10^1 - 10^2$	$10^2 - 10^3$	$10^3 - 10^4$	$10^4 - 10^5$
Thermal	10	11	9	1
$4 \times 10^{-7} - 15$ MeV	0	19	10	2
Total	0	14	14	3



a



b

Figure 1. Differential neutron energy spectra measured in the vicinity of the pressure vessel on the operating floor: a) differential energy spectra; b) cumulative percentage of neutron flux, absorbed dose and dose-equivalent rates versus the neutron energy.

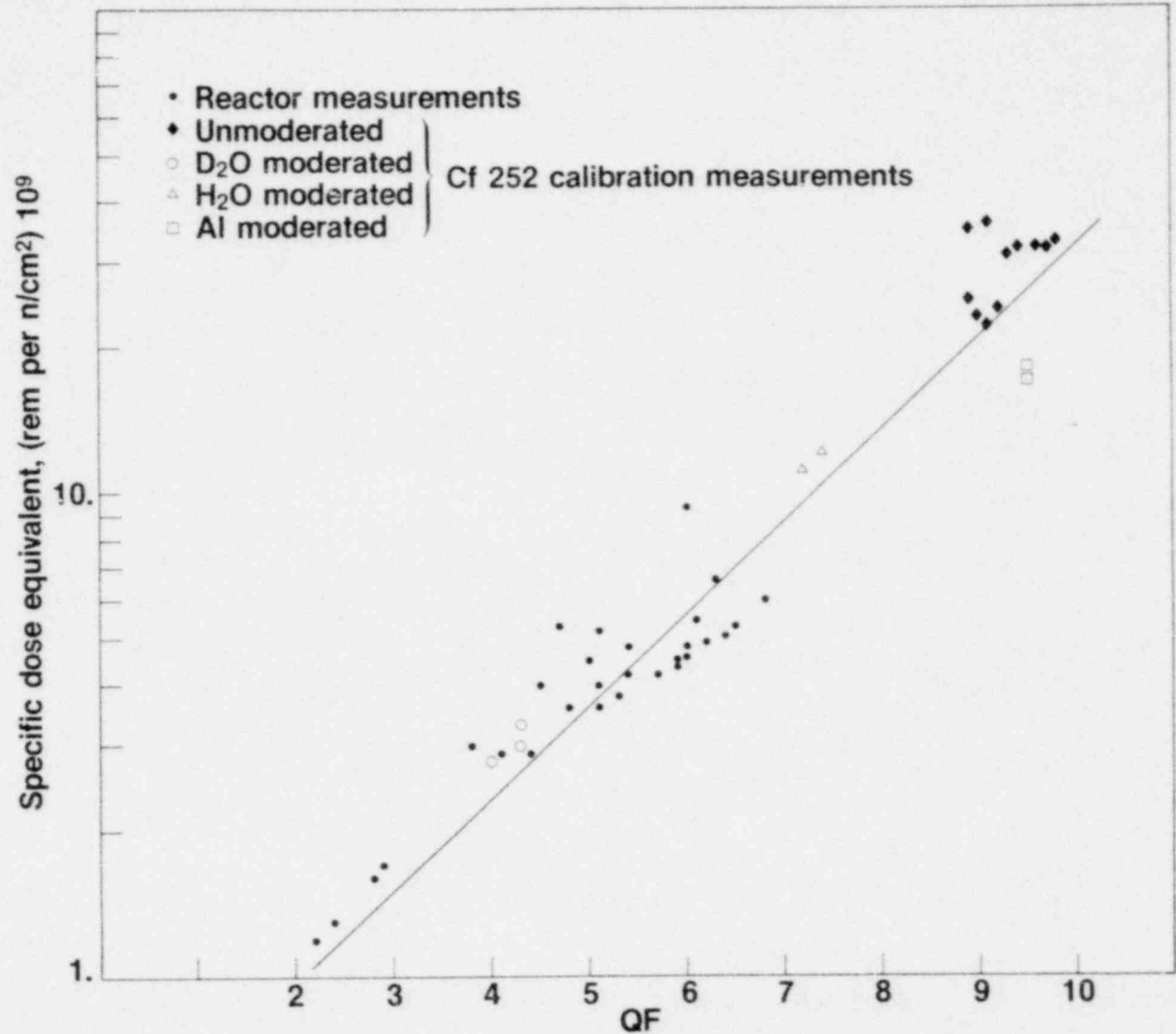


Figure 2. The specific dose-equivalent values versus the quality factors, QF. The solid line is the linear regression curve.

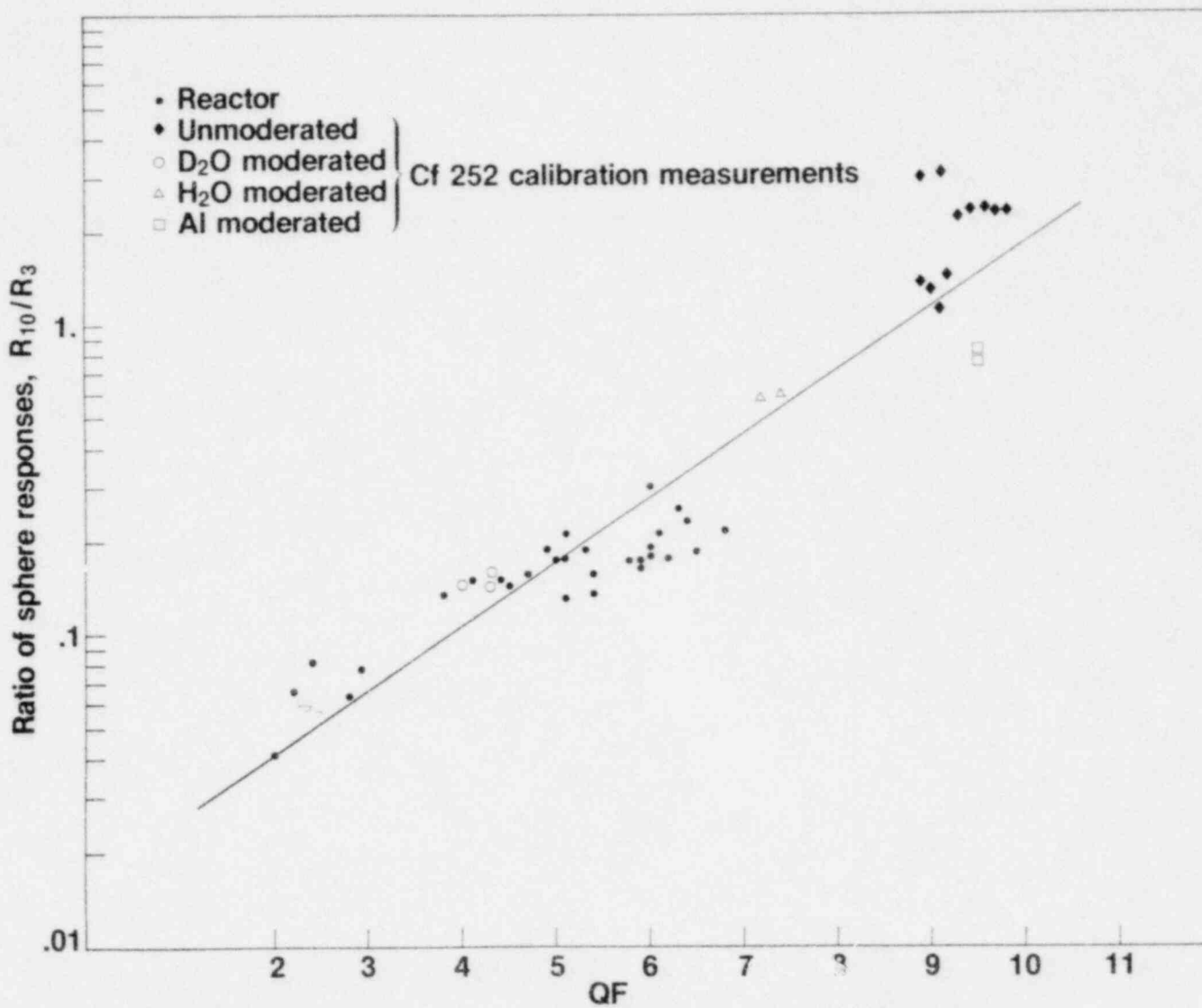


Figure 3. The ratios of 10 in. and 3 in. sphere responses, R_{10}/R_3 , versus the quality factor, QF. The solid line is the linear regression curve.

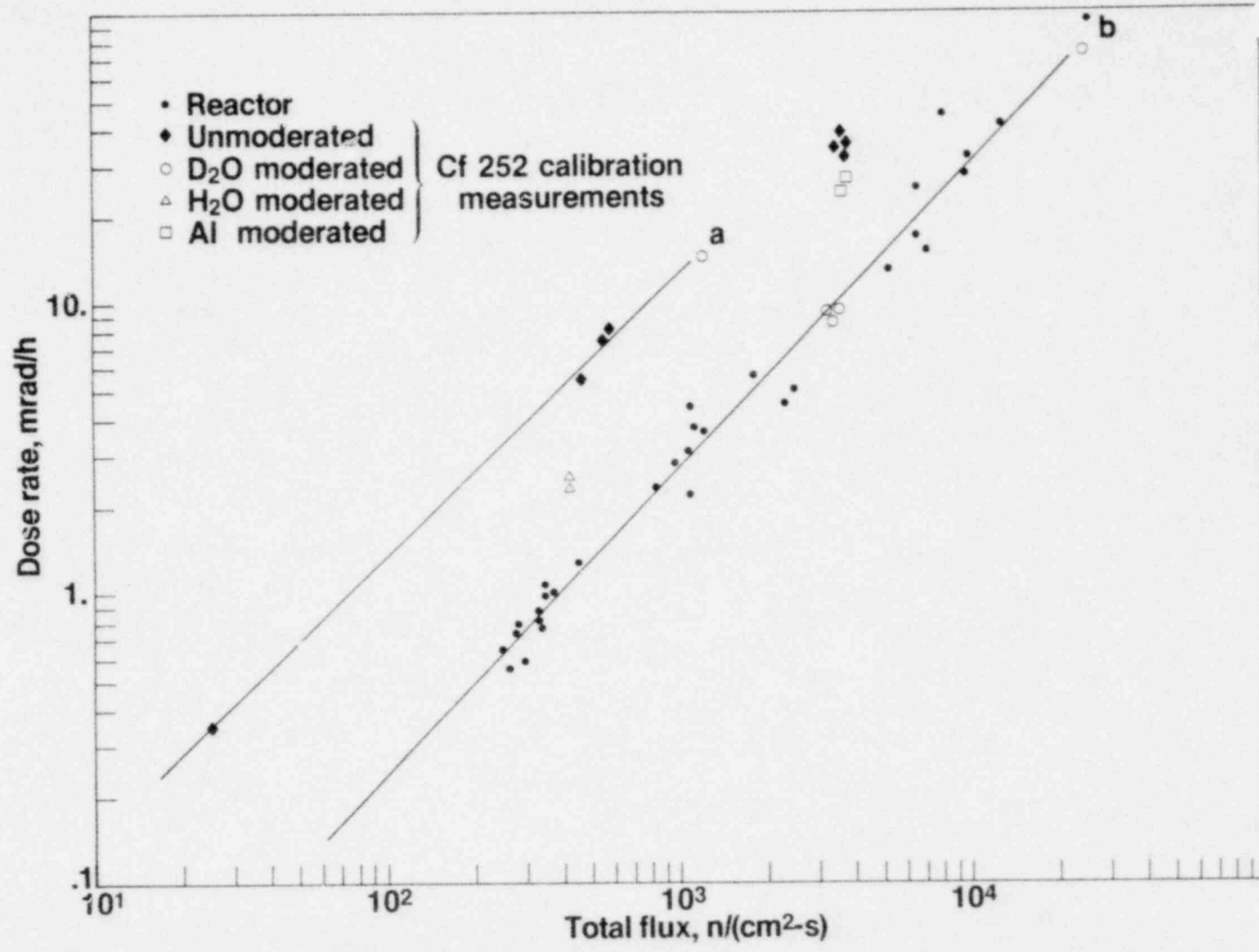


Figure 4. Dose rate versus the total flux of neutrons: line a - from unmoderated ²⁵²Cf fission sources, line b - in the containments of the reactors plus D₂O-moderated fission source.

POOR ORIGINAL

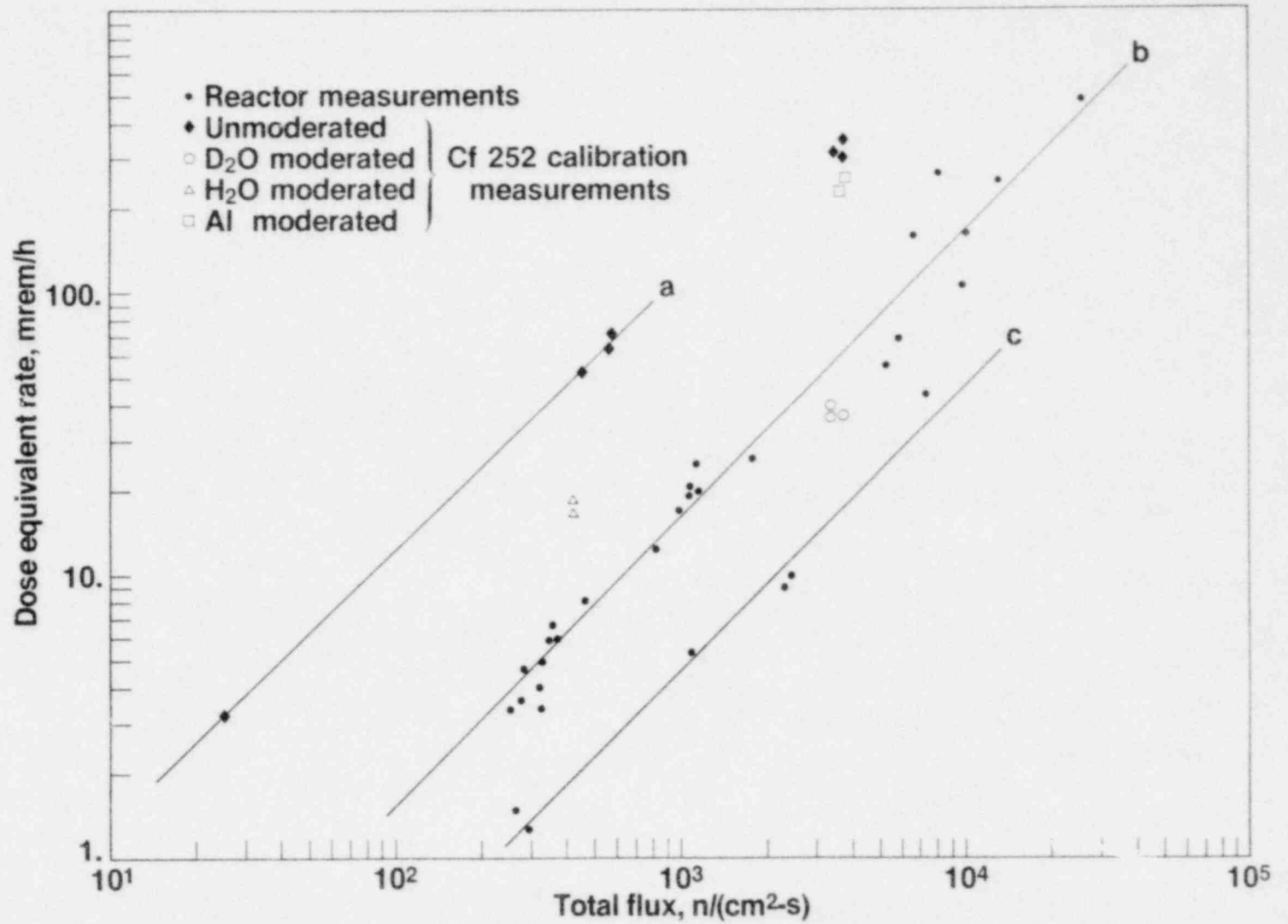


Figure 5. Dose-equivalent rate versus the total flux of unmoderated ^{252}Cf fission sources, line a; the reactor measurements on the operating floor level plus the D_2O moderated fission source, line b, and the reactor measurements on the medium floor level, line c.